Available online at www.sciencedirect.com
SCIENCE DIRECT®
Tectonophysics 366 (2003) 241–258
TECTONOPHYSICS
www.elsevier.com/locate/tecto

Anisotropy of magnetic susceptibility of heated rocks

Bernard Henry[a,*], Diana Jordanova[b], Neli Jordanova[b], Christine Souque[c], Philippe Robion[c]

[a] *Paléomagnétisme et Géomagnétisme, IPGP and CNRS, 4 avenue de Neptune, 94107 Saint Maur des Fosses cedex, France*
[b] *Geophysical Institute, Bulgarian Academy of Sciences, Acad. G. Bonchev Street, block 3, 1113 Sofia, Bulgaria*
[c] *Département des Sciences de la Terre et de l'Environnement, Cergy-Pontoise University and CNRS, 95031 Cergy cedex, France*

Received 11 July 2002; accepted 17 March 2003

Abstract

Heating produces changes, which does not always correspond to simple enhancement of the magnetic fabric. Two methods are proposed to determine the anisotropy of magnetic susceptibility of the ferrimagnetic minerals formed or that have disappeared by chemical change during successive heating. The first diagonalizes the tensor from the difference between each tensor term before and after heating. The second employs linear regression for each tensor term made with the values obtained throughout a thermal treatment. When the same magnetic fabric is obtained from several thermal steps, it cannot be related to randomly oriented ferrimagnetic minerals. Instead, the newly formed fabric must be related to characteristics of the pre-existing rock. By comparing this ferrimagnetic minerals fabric with the initial whole rock fabric, we can distinguish cases where heating simply enhances pre-existing fabric from those where thermal treatment induces a different fabric. Relative to the pre-heating fabric, this different fabric may simply be an inverse fabric or one whose principal susceptibility axes are oriented in a different direction, related to petrostructural elements other than those defining the initial fabric.

Keywords: Anisotropy; Magnetic susceptibility; Thermal treatment; Ferrimagnetic minerals

1. Introduction

Anisotropy of magnetic susceptibility is used to understand rock fabrics. This technique is normally applied on a "fresh" rock, i.e. before any treatment. However, laboratory heating has been used to modify the magnetic fabric of rocks in order to yield more information on their petrofabrics. There are a few problems associated with this technique. One is to determine what is actually modified in the rock. A second is related to the fact that the post-heating fabric is a composite one, resulting from the initial fabric and a new fabric related to the products of mineralogical changes. The aim of the present work is to better understand how magnetic fabric evolves during the heating and above all to isolate the component modified during a thermal treatment.

* Corresponding author. Fax: +33-145-11-4190.
E-mail addresses: henry@ipgp.jussieu.fr (B. Henry), vanedi@geophys.bas.bg (D. Jordanova), vanedi@geophys.bas.bg (N. Jordanova).

0040-1951/03/$ - see front matter © 2003 Elsevier Science B.V. All rights reserved.
doi:10.1016/S0040-1951(03)00099-4

2. Effects of heating on magnetic characteristics of rocks

2.1. Mineral transformations and induced changes in magnetic domain state as a result of heating

During heating, the minerals can be affected by mineralogical changes. However, for the dia- and paramagnetic minerals, these changes have very limited effects on their susceptibility and its anisotropy, except if new ferrimagnetic minerals were formed from these dia- and paramagnetics. On the contrary, susceptibility and anisotropy of pre-existing ferrimagnetic minerals can be radically changed.

An increase of the susceptibility during heating is mainly due to growth of iron oxides. A decrease could be often due to a transformation of these oxides, for example by oxidation of magnetite to hematite. In a recent study of biotite granites, Trincade et al. (2001) pointed out a magnetite growth between 500 and 725 °C (susceptibility increase) and hematization of the magnetite at higher temperature, which caused significant decrease in susceptibility. The magnetic oxides can be generated from iron sulfides (pyrite, pyrrhotite, greigite, troilite), carbonates (siderite, ankerite), silicates, other iron oxides or hydroxides (e.g. Schwartz and Vaughan, 1972; Dekkers 1990a,b). It has been shown that, during heating, hexagonal pyrrhotite (antiferromagnetic) can transform first to monoclinic pyrrhotite (ferrimagnetic) by its partial oxidation to magnetite (Bina et al., 1991). This monoclinic pyrrhotite resulted from Fe/S ratio equilibrium and causes a significant change in the susceptibility. At higher temperatures, pyrrhotite oxidizes mostly to magnetite. Siderite oxidizes to magnetite or maghemite, even at room temperature when exposed to air for periods of weeks to months, and even faster during heating (Ellwood et al., 1986; Hirt and Gehring, 1991). Exsolved magnetite has been observed in plagioclase, pyroxene and mica. Maghemite inverts to hematite in the temperature range from 250 to 750 °C, depending on the grain size, degree of oxidation and incorporation of impurity ions in the crystallographic lattice (Verwey, 1935; Özdemir, 1990). Goethite dehydrates in the range 250–370 °C to form usually hematite, generally in very fine grains (Gehring and Heller, 1989; Dekkers, 1990b). Lepidocrocite starts to transform to superparamagnetic (SP) maghemite at ~ 175 °C but the structural transformation is completed around 300 °C with further conversion of this maghemite to hematite (Gehring and Hofmeister, 1994). In an oxidizing atmosphere, ferrihydrite transforms to hematite, which is accompanied by the reduction of specific surface area and microporosity (Weidler and Stanjek, 1998). In contrast, heating ferrihydrite in the presence of organic reductant (e.g. glucose, charcoal) leads to formation of magnetite and/or maghemite, or magnetite/maghemite intermediates (Campbell et al., 1997).

Important rock constituents are the phyllosilicates. With increasing temperature they undergo the following reactions (Murad and Wagner, 1998): (i) loss of physically adsorbed or intercalated water at 100–200 °C; (ii) oxidation of Fe^{2+}; (iii) loss of structural hydroxyl between about 400 and 550 °C; (iv) final structural breakdown combined with the formation of new phases close to 1000 °C; (v) vitrification. The type of the phases that develop at high temperatures depends on the composition of the original clay minerals, the firing temperature and oxygen activity, in which the clay is heated. The iron that cannot be accommodated in silicate structures during heating in oxidizing conditions reacts with oxygen to form SP hematite grains at high temperatures. In a system of clay matrix and mineral phases, increasing temperature leads to a progressive welding between clay matrix and mineral, shape changes of mineral phases, increase of the aggregation rate within the clay matrix with formation of secondary porosity and ''intergranular bridges'' (Riccardi et al., 1999). A mixture of natural clays and micas or calcite undergoes structural breakdown starting from ~ 550°, while in a mixture with quartz or albite, no appreciable morphological and chemical transformations occur until ~ 1000 °C. On the other hand, magnetic properties of the ferrimagnetic phases embedded into a clay matrix are also influenced by the type of phyllosilicates present (Osipov, 1978). For example, the inversion temperature of maghemite to hematite is ~ 250 °C when kaolinite predominates in the clay minerals, while the conversion temperature is shifted to 400–450 °C when a bentonite matrix is present and further up to ~ 500 °C with a mica-rich matrix (Osipov, 1978).

As a result of laboratory thermal treatment, ferrimagnetic minerals are prone not only to chemical and structural transformations mentioned above, but also to changes in effective magnetic grain size through grain

growth or alteration. Grain size dependence of magnetic susceptibility is weak for Pseudo Single-Domain (PSD) and Multi-Domain (MD) magnetite grains (Hartstra, 1982), but becomes important if the grain size variation corresponds to transformation SP–Single-Domain (SD) or SD–PSD–MD. The susceptibility of the SD grains is lower in comparison with SP, PSD and MD sizes (Stacey and Banerjee, 1974).

Magnetic annealing effects can also play a significant role through homogenization of the distribution of crystal defects, thus leading to an increase in the susceptibility of large grains and redistribution of domain wall pining sites in the crystals. One of the causes of significant susceptibility variation is the inversion by filling up by new cations of the vacancy sites within the crystal lattice (Bina and Henry, 1990). This last mechanism is accelerated by heating, and could be at the origin of susceptibility increase during heating even at relatively low temperatures.

2.2. Variations in anisotropy of susceptibility

In a number of publications, modification of the magnetic fabric as a result of heating has been applied to different types of rocks (e.g. Abouzakhm and Tarling, 1975; Kropacek, 1976; Urrutia-Fucugauchi, 1981; Schultz-Krutisch and Heller, 1985; Peraneau and Tarling, 1985; Ellwood et al., 1986; Jelenska and Kadziako-Hofmokl, 1990; Hirt and Gehring, 1991; Xu et al., 1991; Li et al., 1998; Borradaile and Lagroix, 2000; Trincade et al., 2001; Souque et al., 2002). The outcome was sometimes a simple enhancement of the fabric, but significant changes of the fabric have also been obtained.

In many cases, the majority of the minerals that contribute to the initial fabric (F_0) are only marginally transformed during heating, and the effect of the heating can therefore be considered as limited to the creation of a new fabric (F_n) carried by ferrimagnetic minerals. The result is then a composite fabric (F_0+F_n), with F_n either relatively similar or different from F_0. If the carriers of the initial fabric are significantly altered during heating, F_0 can loose a part F_l. The simplest case is when F_l occurs in the absence of F_n and is more complex when F_n is created at the same time, the composite fabric being ($F_0-F_l+F_n$). During subsequent heating to some maximum temperature, the fabrics F_n and F_l can be enhanced by an increase (by a factor p different according to the heating steps) of the same mineralogical alterations (F_0+pF_n or F_0-pF_l), or may become more complex due to transformations of other minerals, which give different fabrics F_l', F_n', etc. It is clear that a fabric like $F_0-F_l-F_l'+F_n+F_n'+\ldots$ will be very complex and hardly interpretable. On the contrary, if the composite fabric can fit to a model F_0+pF_n or F_0-pF_l with only a variation of p for different applied temperature, the evolution of the composite fabric is straightforward because a same magnetic fabric is added or lost during the different steps. The aim of the methods proposed here is to recognize this case and then to determine the characteristics of the fabric F_n or F_l.

3. New approaches for analyzing the magnetic fabric of heated rocks

3.1. Partial magnetic fabrics

In the first approach, we analyze the partial magnetic fabric that appears or disappears during thermal treatment. The initial fabric being not significantly modified during heating, these partial fabrics correspond only to the fabric carried by the newly formed or disappeared ferrimagnetic minerals. Such a partial fabric, developed between fabrics F_1 and F_2, measured respectively after heating at temperatures T_1 and T_2 ($T_2>T_1$), can be easily determined by diagonalization of the tensor F_{12}, which is determined by subtracting the tensors corresponding to the fabrics F_1 and F_2.

$$F_1=\begin{vmatrix} xx_1 & xy_1 & xz_1 \\ yx_1 & yy_1 & yz_1 \\ zx_1 & zy_1 & zz_1 \end{vmatrix}$$

$$F_2=\begin{vmatrix} xx_2 & xy_2 & xz_2 \\ yx_2 & yy_2 & yz_2 \\ zx_2 & zy_2 & zz_2 \end{vmatrix}$$

$$F_{12}=\begin{vmatrix} xx_1-xx_2 & xy_1-xy_2 & xz_1-xz_2 \\ yx_1-yx_2 & yy_1-yy_2 & yz_1-yz_2 \\ zx_1-zx_2 & zy_1-zy_2 & zz_1-zz_2 \end{vmatrix}$$

Table 1
Pre-heated samples characteristics

Rock type / Locality / Sample	Rockmagnetic properties	Initial magnetic mineralogy / K (10^{-6} SI)
Quartz-monzogabbro Elshitsa Pluton–SW Bulgaria b1	Curves of thermal demagnetization of Natural Remanent Magnetization (NRM) is characterized by a concave shape, corresponding to coarse magnetically soft ferrimagnetic carriers. Thermomagnetic analysis of low field susceptibility $K(T)$ shows a sharp decrease (Fig. 1) at the Curie temperature (T_c) of pure magnetite (580 °C). A weak susceptibility decrease around 350 °C is also present, probably indicating alteration of a minor pyrrhotite. The characteristic rectangular shape of the $K(T)$ curve and the absence of a well expressed Hopkinson peak suggest that the magnetite is of large MD size.	Fe_3O_4 + traces of pyrrhotite 43,225
Amphibole-biotite granodiorite Elshitsa Pluton–SW Bulgaria b2		Fe_3O_4 + traces of pyrrhotite 9995
Gabbro Plana Pluton–SW Bulgaria b3		Fe_3O_4 97,028
Diorite Plana Pluton–SW Bulgaria b4		Fe_3O_4 27,969
Granite Cerro Mirador Pluton– Livingston Island–Antarctica c1, c2	Thermomagnetic $K(T)$ analysis (Fig. 1) shows two decreases of susceptibility—magnetite T_c and a second decrease around 350 °C. This second variation is not visible on the cooling curve. Thermal demagnetization of the NRM and of Saturation Isothermal Remanent Magnetization (SIRM) suggest that pyrrhotite is the main NRM carrier (in this case a TRM), probably of stable SD-PSD size in samples c1 and c2. Some magnetite contribution is also visible, with higher contribution to samples c3 and c4.	Mixture Fe_3O_4 + pyrrhotite 1994, 309
Granite Hesperides Pluton–Livingston Island–Antarctica c3, c4		Mixture Fe_3O_4+ pyrrhotite 39,178; 18,751
Volcanoclastic sediment Eastern Rhodopes–Bulgaria d1	A well expressed Hopkinson peak of a titanomagnetite with $T_c \sim 430$ °C is evident, as well as a titanomagnetite with composition, closer to that of magnetite with a T_c of ~ 500 °C (Fig. 1). T_c of ~ 650 °C is also detected. The cooling curve shows decrease in K, probably connected with the formation of hematite at high temperatures. Rock-magnetic studies (Karloukovski, 2000) suggest that the ferrimagnetic minerals are mainly of PSD grain size. Low SP content (Xfd% = 2.3 %) is also reported.	Titanomagnetite, Fe_3O_4 4045
Ignimbrite Eastern Rhodopes–Bulgaria e1	The sample contains andesitic xenoliths of varying sizes. High-temperature behavior of magnetic susceptibility (Fig. 1) shows presence of titanomagnetite with a T_c of ~ 500–550 °C, but also of some highly oxidized magnetite. The cooling curve shows a decrease in K, probably connected with the formation of hematite at high temperatures. Hysteresis measurements carried out by Karloukovski (2000) indicate MD grain size.	Fe_3O_4, titanomagnetite 11,355
Limestone Corbières–France level 1: a1–a5, a11, a15, a19, a21	Souque et al. (2002) used different rock-magnetic techniques to study these samples. From Lowrie (1990), thermomagnetic (susceptibility in low field) and hysteresis experiments, they observed the presence of minerals with low-medium coercivity (magnetite) and high coercivity (hematite). Magnetite appears to have a wide grain size distribution. Thermomagnetic curves underline the strongly dominant contribution of magnetite to the susceptibility.	Fe_3O_4 + traces of αFe_2O_3 150–193
Limestone Corbières–France level 2: a6–a9, a22, a23, a25		Fe_3O_4 + traces of αFe_2O_3 55–71
Loess sediments (non-weathered silty loess) Russe–Bulgaria f1, f2	Thermomagnetic $K(T)$ analysis (Fig. 1) shows that the main ferrimagnetic phase is magnetite, also with some hematite fraction (T_c of 680 °C). After heating up to 700 °C, a significant susceptibility increase suggests the formation of large amounts of secondary magnetite (Fig. 1).	Fe_3O_4 + αFe_2O_3? 328; 276

Table 1 (*continued*)

Rock type Locality Sample	Rockmagnetic properties	Initial magnetic mineralogy K (10^{-6} SI)
Loess (mixed with volcanic ash) Tönchesberg–Germany g1, g2	Thermomagnetic $K(T)$ analysis (Fig. 1) shows that the main ferrimagnetic phase is magnetite. These samples are characterized by a second phase with T_c of 250 °C, which can be attributed to titanomagnetite grains present into the volcanic elements mixed with the primary loess material (Hus and Jordanova, 1996). After heating to 700 °C, a significant increase of susceptibility indicates the formation of large amounts of secondary magnetite (Fig. 1).	Fe_3O_4 + Titanomagnetite 741; 677
Pliocene clay sediment Pleven–N Bulgaria h1	Thermomagnetic $K(T)$ analysis points out only traces of magnetite. SIRM alternating field (AF) demagnetization shows the presence of a high coercivity component (goethite?).	Traces Fe_3O_4 105

The main problem with this approach is that, to be significant, the difference of the tensor terms has to be much larger than the uncertainty in the value of the terms of each tensor. Unfortunately, it seems difficult to define a reliable criterion for this significance level. Looking at the particular case of a diagonalized tensor, the difference F_{12} for the diagonal term could be compared to the uncertainty in each individual diagonal F_1 and F_2 term, but not for the symmetrical terms (e.g. a zero difference for the latter does not mean a non-significant result).

It is also clear that F_{12} and F_{21} are different, and that we have to introduce conditions for the choice between F_{12} and F_{21}. Negative tensor terms $xx_1 - xx_2$, $yy_1 - yy_2$ and $zz_1 - zz_2$ should result from diagonalization of a diamagnetic fabric. If these terms are very small, such a fabric should be real, but, owing to the uncertainty, the method will not give reliable results in such a case. We have therefore to choose between F_{12} and F_{21} the case with positive values for all the differences of the diagonal terms of the tensors F_1 and F_2. When mean susceptibility decreases, the change in fabric arises from the disappearance of ferrimagnetic minerals (i.e. converted to non- or less magnetic phases). When mean susceptibility increases, the fabric is related to newly formed ferrimagnetic minerals (i.e. converted from non- or less magnetic phases). The principal values of the tensor represent only the differences in susceptibility, but without knowledge of the actual susceptibility (amount of newly formed minerals unknown).

If the evolution of the magnetic fabric corresponds exactly to the model $F_0 + pF_n$ or $F_0 - pF_l$ with varying p for heating steps at increasing temperature, the normalized tensor differences obtained for temperatures $T_0 - T_1$, $T_0 - T_2$, $T_0 - T_3$, $T_1 - T_2$, $T_1 - T_3$, $T_2 - T_3$, etc., have similar principal axes orientation and shape. We thus studied the mean tensor obtained from the tensor differences $T_0 - T_1$, $T_1 - T_2$, $T_2 - T_3$, without normalizing by the mean susceptibility, and we determined the confidence zone for each principal axis by statistical methods (Hext, 1963; Jelinek, 1978; Constable and Tauxe, 1990; Henry, 1997). This method is valid even for a single heating step, but obviously in this case without any possibility to control if the fabric change can be described by models $F_0 + pF_n$ or $F_0 - pF_l$.

3.2. Linear regression

The models $F_0 + pF_n$ or $F_0 - pF_l$ correspond precisely to the basic hypotheses of the linear regression method (Henry, 1983; Henry and Daly, 1983). They are (1) presence of two components, and (2) one component considered as in constant proportion and with a moderate susceptibility, and the other of very high susceptibility in varying amount (giving thus varying mean susceptibility). Here, we do not use the data from different samples, but from the same sample after different treatments. The results obtained using the slope from the linear regressions in this case concern only the newly formed or those that have disappeared minerals with very high susceptibility, i.e. here the ferrimagnetic minerals.

Uncertainty in the slope derived from the linear regression contributes to the uncertainty window for each tensor term and here we employ the bootstrap (Efron, 1982; Efron and Tibshirani, 1986) method to estimate the confidence zone at 95% significance. For each bootstrap resampling (here 10,000 iterations), each tensor term (slope value from the linear regression) used in the diagonalization was chosen randomly within its uncertainty window (parametric bootstrap; Tauxe and Watson, 1994). The retained confidence zone at 95% for each principal axis and for the P' and T parameters in the Jelinek (1981) diagram is the maximum density contour containing 95% (here 9500) bootstrap results.

Under conditions that mean susceptibility has regular variation (i.e. not limited to a change from values all close to a mean susceptibility K_{m1} to values all close to a mean susceptibility K_{m2}), well defined linear regressions (i.e. when correlation coefficient r is close to 1 or -1) obtained using tensors T_0, T_1, T_2, T_3,..., indicate that the variation of the magnetic fabric during heating could be modeled using F_0+pF_n or F_0-pF_l. On the contrary, incoherent tensor terms variations yield the assumption of F_0+pF_n or F_0-pF_l invalid.

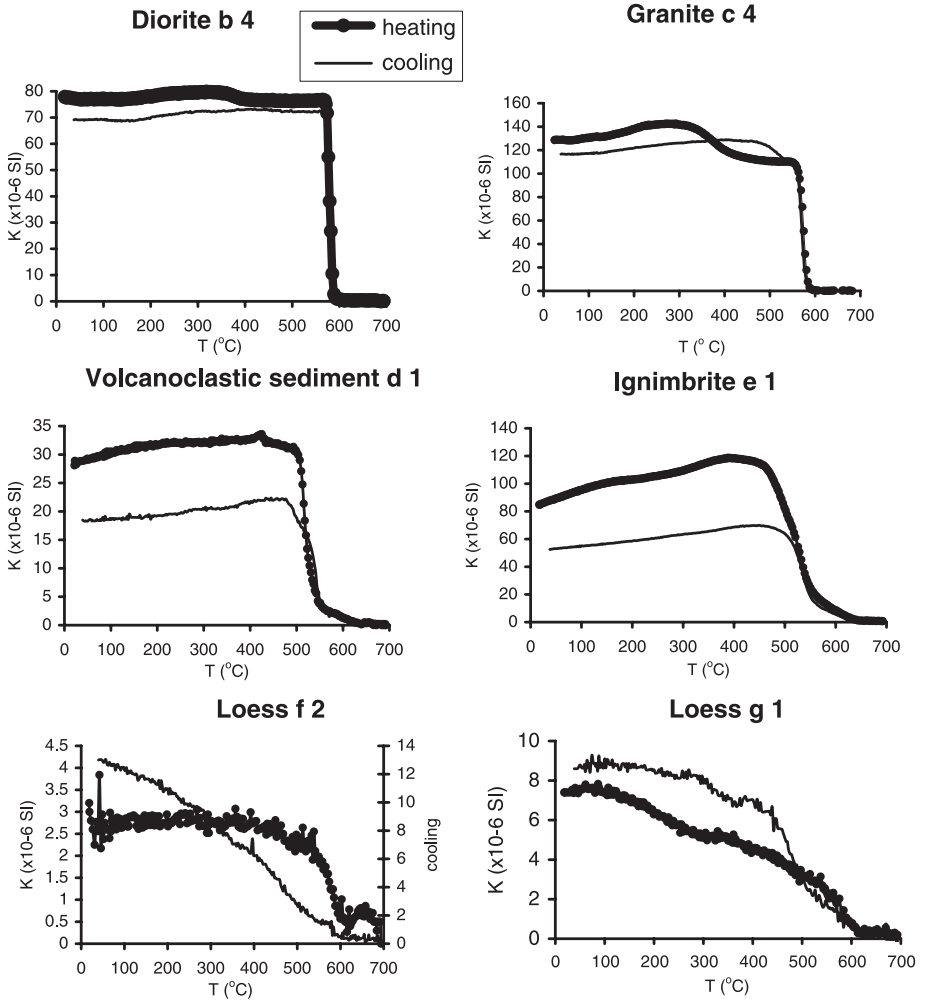

Fig. 1. Thermomagnetic analysis of magnetic susceptibility for samples b4, c4, d1, e1, f2 and g1. Heating in air.

4. Applications

This new approach was tested in practice by studying a collection of different rock samples heated stepwise up to 500° (limestone studied in the Cergy-Pontoise laboratory) or 700 °C (other samples studied in the Sofia laboratory). Information about the source, rock type and initial magnetic mineralogy and susceptibility is given in Table 1.

4.1. Sample description and main sources of the initial AMS fabric (Table 1)

4.1.1. Plutonic rocks

Samples b1–b4 from granitic plutons from SW Bulgaria show generally high values of magnetic susceptibility, suggesting that their magnetic fabric is determined mainly by the contribution of the ferrimagnetic fraction. An exception is sample b2, which shows relatively low magnetic susceptibility. The main magnetic carrier is MD magnetite and traces of pyrrhotite. *Granites from Livingston Island* (samples c1–c4) come from two different plutonic bodies and have variable values of magnetic susceptibility (Table 1). The main ferrimagnetic minerals are pyrrhotite and magnetite.

4.1.2. Sediments

Seventeen *limestone samples* (a_n), were taken from two beds (levels 1 and 2) from a single outcrop. Souque et al. (2002) found the presence of magnetite with traces of hematite in these samples. Four samples from *loess sediments* (f1, f2, g1, g2) were also studied. The main ferrimagnetic phase is magnetite, although the Bulgarian loess samples (f1, f2) contain a minor hematite fraction as well. Loess samples from Tönchesberg (g1, g2) probably contain some titanomagnetite. *Sample d1* comes from Miocene sedimentary deposits in Eastern Rhodopes (Bulgaria). The main ferromagnetic mineral is titanomagnetite (Karloukovski, 2000). *Sample h1* is taken from the Upper Pliocene base complex in NW Bulgaria. It contains traces of magnetite, and perhaps of goethite.

4.1.3. Volcanic rocks

Sample e1, from Miocene formation in Eastern Rhodopes (Bulgaria), is taken from a pyroclastic flow, containing predominantly magnetite of MD grain size (Karloukovski, 2000).

Thermomagnetic experiments show different degrees of change in the magnetic mineralogy (Fig. 1). Details about the studied samples and their rock-magnetic properties are given in Table 1.

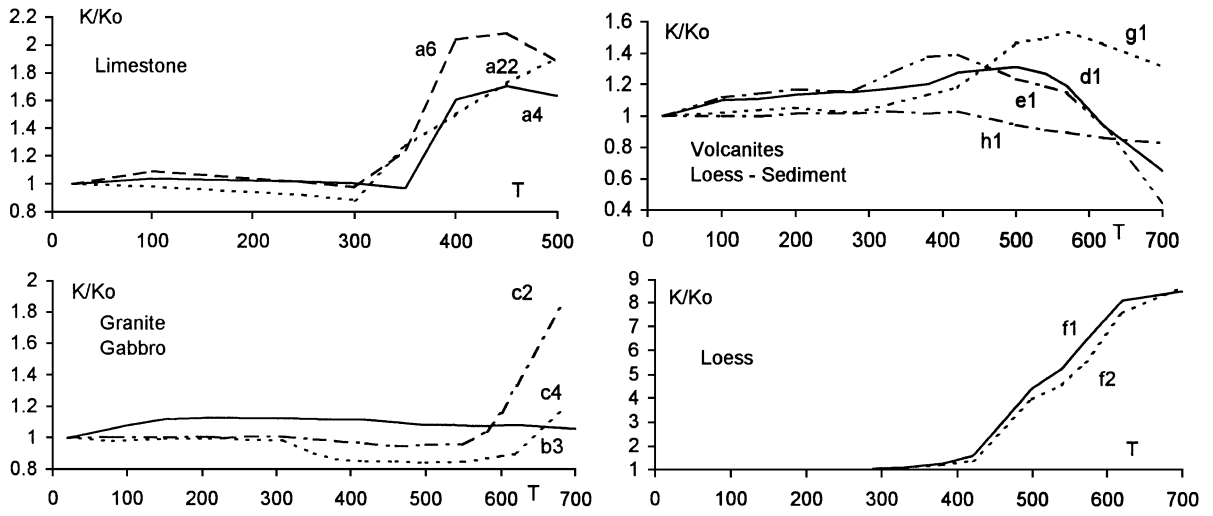

Fig. 2. Relative variation of the susceptibility at room temperature K/K_o as a function of the maximum temperature T (°C) applied, for some of the studied samples.

4.2. Susceptibility variations during stepwise heating

Fig. 2 illustrates examples of variations of the mean susceptibility during heating normalized by the original non-heated values. Most samples (18 of 24) show no significant variation below 300–400 °C. Above these temperatures, these samples exhibit variable susceptibility changes ranging from strong increase (f1 and f2), increase mostly followed by stabilization (most of the limestones) or decrease (g1 and g2, part of the limestones), weak decrease followed by increase (c1–c4), and decrease (h1). Samples (b1–b4, d1 and e1) have increasing susceptibility for initial lower temperature steps and more or less important decrease for higher temperature steps.

As marked variations in absolute susceptibility value are necessary for obtaining significant results, data for sample h1 and often for the temperature range in which susceptibility decreases, do not meet the necessary criterion (see Fig. 3). For better determining the chemical/phase transformations, a method developed by Van Velzen and Zijderveld (1992) was applied to eight samples (b2, b3, c4, d1, e1, f2, g1, h1) representative of the different magnetic behaviors (see examples on Fig. 4). The results are briefly summarized in Table 2. The mineralogical changes

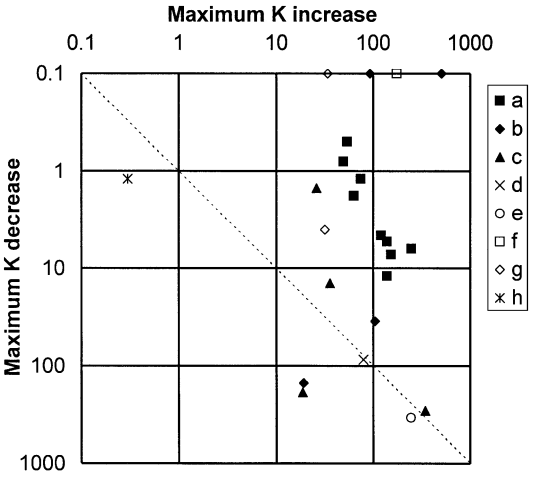

Fig. 3. Maximum susceptibility (K) total decrease relative to initial susceptibility, shown as a function of the corresponding increase, for the studied samples. Susceptibility K in 10^{-6} SI (data with value 0 are presented here as value 0.1, because of logarithmic scale). For most samples, increase is much stronger than decrease.

are mostly due to the formation of magnetite above 300 °C and of hematite above 500–600 °C. Magnetic grain sizes also changed. For the samples showing both sufficient decrease and increase of susceptibility, we separated AMS variation associated to decrease from that related to increase.

4.3. Comparison of the data obtained by tensor difference and linear regression

Often, the results obtained by tensor difference are relatively scattered, because of the small differences between the tensor values for different heating steps. Fig. 5 shows examples of the directional changes observed for the principal axes. The relative scattering does not allow testing whether the fabric change corresponds or not to models F_0+pF_n or F_0-pF_l.

Fig. 6 presents an example of the regressions for symmetrical tensor term obtained for sample c4, for decrease and increase of susceptibility. The quality of regressions for the diagonal term is not a significant criterion, correlation coefficient r being always very high. The r-values higher than 0.99 indicate that the quality of regression is excellent, thus satisfying the criterion for the models F_0+pF_n and F_0-pF_l. Non-perfect linear arrangement occurs mostly at the highest temperature step(s) for the other samples. A selection has been therefore made to have only high quality (r close to 1 or -1) linear regression. Regression quality is a little lower for the limestones compared to the other samples.

A comparison of the tensor difference and linear regression methods was made using the same data, exhibiting significant regression. The mean tensor derived from the tensor differences agrees very well with the results obtained by linear regression, including for the anisotropy degree $P'=\exp\sqrt{2[(n_1-n_m)^2+(n_2-n_m)^2+(n_3-n_m)^2]}$ and the shape parameter $T=[2(n_2-n_3)/(n_1-n_2)]-1$ (where $n_i=\ln K_i$, K_i are the principal susceptibility values $K_1\geq K_2\geq K_3$ and K_m the geometric mean of the principal susceptibility values; Jelinek, 1981). Contrary to the linear regression method, the tensor difference approach does not imply that the mineralogical changes concern high susceptibility minerals. The agreement of the results from the two approaches therefore confirms that the AMS changes

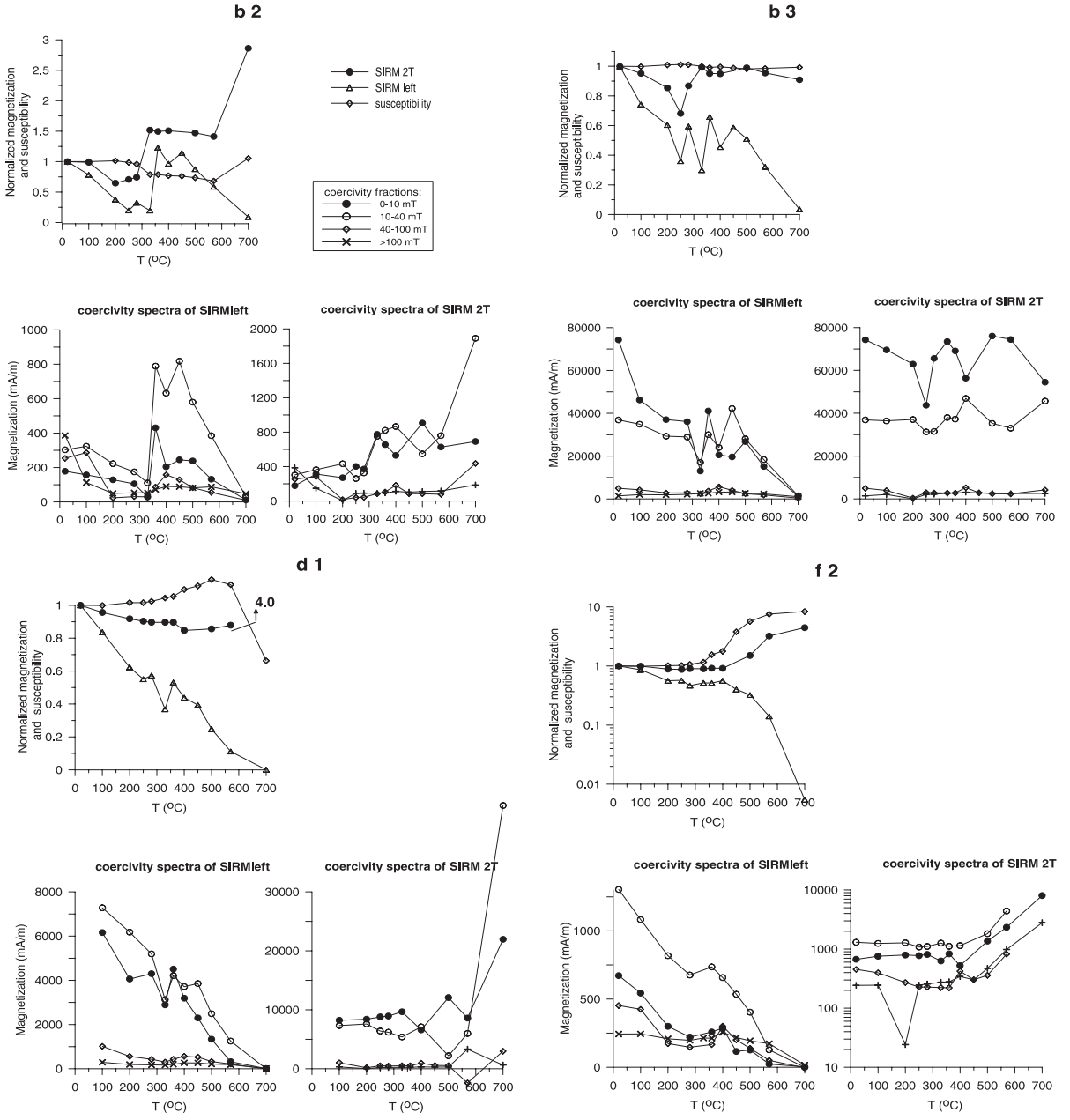

Fig. 4. Example of the results from the experiment to detect mineralogical changes during heating for samples b2, b3, d1 and f2. This method, described in detail in Van Velzen and Zijderveld (1992), includes subsequent measurements after each temperature step of the following parameters: (1) SIRM (2T) acquired in each previous step-referred to as SIRMleft, (2) magnetic susceptibility *K*; (3) SIRM(2T) imparted after each temperature step; (4) coercivity spectra of SIRMleft and SIRM(2T) obtained by an AF demagnetization at 10, 40 and 100 mT maximum AF amplitude. As a result, for each sample are obtained: thermal demagnetization decay curves of SIRMleft, decay curves of the coercivity fractions (0–10 mT), (10–40 mT), (40–100 mT) and (>100 mT) of the SIRMleft and of SIRM2T, as well as variations of the full SIRM2T, induced after each temperature step, and of the magnetic susceptibility.

Table 2
New Fabric

Sample	Mineralogical alterations	Comparison of the F fabric (formed or destroyed ferrimagnetic minerals) with the F_0 fabric (whole rock)
b1–b4	(b2) After about 300 °C, formation of SD–PSD magnetite (new phase corresponding 0–10 and 10–40 mT coercivity fraction; Fig. 4) from coarse grained pyrrhotite (the decrease of susceptibility is probably related to variation of grain size). After the 580 °C step, formation of hematite (increase of the high coercivity fraction), probably from magnetite and, at the same time, occurrence of new magnetite (increase of K and SIRM2T). (b3) Despite the quite stable behavior of magnetic susceptibility during step-wise heating (Fig. 2), SIRM2T curve suggests that certain transformations, not clearly identified, occur in the temperature interval 200–500 °C.	Samples b1 to b4 show only slight differences in the orientation of the principal axes. However, for b1 and b2 samples, confidence zones are small for the F_0 (related to measurement) and F fabrics; these confidence zones do not overlap. The axes directions are therefore significantly different at least in these two samples. The shape parameter values are different in F and F_0 fabrics for all four samples. The P' values for the F fabric are significantly higher than for the F_0 fabric.
c1–c4	(c4) Mineralogical alterations similar to the ones obtained for sample b2. Magnetite (formed after 300 °C heating) is however of lower coercivity than in b2.	Samples c1, c3 and c4 present sufficient variation of susceptibility to separate fabrics associated with a decrease (F_l) and an increase (F_n) of susceptibility. The axis directions are different in fabrics F_l, F_n and F_0. Owing to the small size of confidence zone (Fig. 5), these differences are significant for at least part of the axes. Sample c2 yields only a F_n fabric, with small confidences zones. All the axes are significantly different for F and F_0 fabrics. In these four samples, shape parameter values are different for the different fabrics, and the P' values are higher for F_l and F_n fabrics than for F_0 fabrics.
d1	(d1) (Fig. 4) Until about 500 °C, the dominant evolution is the formation of SP grains (increase of K and decrease of SIRM2T) whereas at higher temperature, the main change is the occurrence of SD–PSD grains (decrease of K and increase of SIRM2T; dominant coercivity fraction becomes 10–40 mT).	For the F_n and F_l fabrics, axes directions and shape parameters are similar and coincide with the F_0 fabric. P' values are higher for F fabrics.
e1	(e1) Mineralogical alterations similar to those for sample d1, but more strongly developed.	For the F_n and F_l fabrics, axes directions and shape parameters are similar and coincide with the initial F_0 fabric. The difference in orientation of the maximum axes (Fig. 5) is not significant, the confidence zones being overlapping (oblate fabrics). Note, however, the remarkable coincidence of maximum axis for the F_n and F_l fabrics, though determined from different heating steps. P' values are higher for F fabrics.
Level 1 limestones	Formation of magnetite and decrease of the initial hematite content (Souque et al., 2002).	Minimum axes of the F and F_0 fabrics are perpendicular. Maximum axes of the two fabrics have different orientations, but non-perpendicular. Generally the F fabric is prolate and the F_0 fabric oblate (Fig. 8). The P' values are not significantly different in the two fabrics.
Level 2 limestones	Formation of magnetite and decrease of the initial hematite content (Souque et al., 2002).	The maximum and minimum axes are permuted between F and F_0 fabrics (Fig. 7). The F fabric is mostly prolate and the F_0 fabric oblate (Fig. 8). The P' values are not significantly different in the two fabrics.

Table 2 (*continued*)

Sample	Mineralogical alterations	Comparison of the F fabric (formed or destroyed ferrimagnetic minerals) with the F_0 fabric (whole rock)
f1–f2	(f2) From 300 °C upward, as a result of clay alteration (Osipov, 1978; Murad and Wagner, 1998), magnetite grains are formed (Fig. 4), mainly SP until 400 °C (increase of K and decrease of SIRM2T) and larger at higher temperature (increase of K and SIRM2T). From heating at 500 °C upward, part of the magnetite oxidizes to hematite (increase of the high coercivity fraction). Simultaneously new magnetite formation still occurs (increase in intensity of all the coercivity fractions).	Axes directions and shape parameters of the F and F_0 fabrics agree very well. P' values are higher for F fabrics.
g1–g2	(g1) Mineralogical alterations relatively similar to that for the sample f2, except at very high temperature where less magnetite (mainly SD–PSD) is formed together with hematite (increase only of the 10–40 mT and high coercivity fractions).	Axes directions and shape parameters of the F and F_0 fabrics agree very well. P' values are higher for F fabrics.
h1	(h1) The dominant mineralogical alteration is the formation of hematite, probably from goethite and MD magnetite (increase of SIRM2T and decrease of K).	No significant F fabric.

are only related to the contribution from ferrimagnetic minerals. The confidence zones are slightly smaller using the linear regression method, probably because of the possible bias inherent to the tensor difference approach. The two methods give a similar tensor. Therefore, the linear regression method was chosen for the data analyses.

4.4. New fabric—case studies

4.4.1. Comparison of the fabric of ferrimagnetic minerals isolated from heated fabric with the initial AMS fabric

Comparison of the fabric of ferrimagnetic minerals isolated during heating ($F=F_n$ or F_l) with the initial

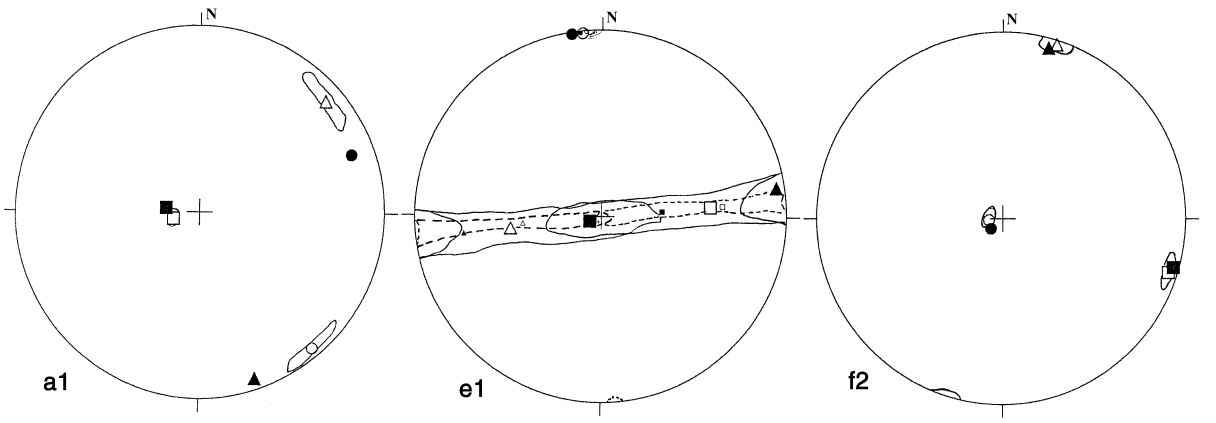

Fig. 5. Maximum (squares) and minimum (circles) susceptibility axes for the mean tensor differences (full symbols) and from the regression method (open symbols) for samples a1, e1 and f2. Associated confidence zones from the regression method. Large (small) symbols and continuous (dashed) line for the confidence zone correspond to increase (decrease) of susceptibility. Stereographic projection in the lower hemisphere.

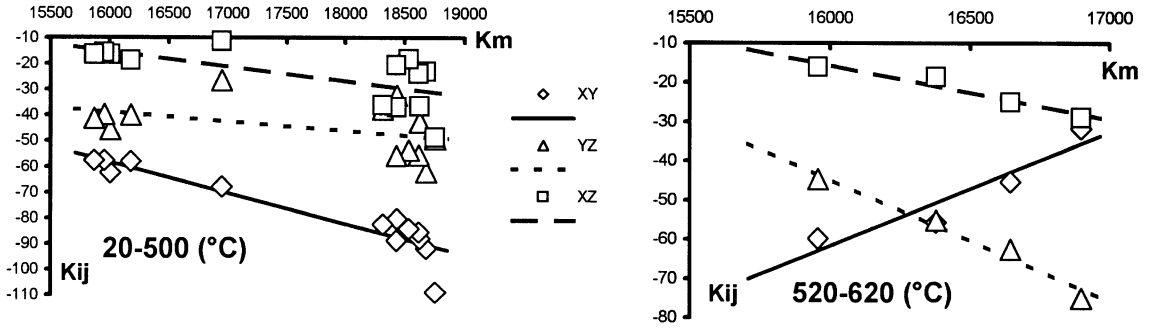

Fig. 6. Linear regressions of the symmetrical tensor terms for the granite sample c4, associated to the decrease (20–500 °C) and increase (520–620 °C) of susceptibility. K_{ij} and K_m in 10^{-6} SI. Note that the scale is very different for the two axes.

AMS fabric (F_0) is shown in Fig. 7. Fig. 8 shows the differences in the degree of anisotropy P' and shape of the ellipsoid T (Jelinek, 1981). Comparison of the F and F_0 fabrics for the studied samples is given in Table 2.

In most cases the F fabric is more anisotropic than the F_0 fabric. Another approach using anisotropy of remanent magnetization to determine the ferrimagnetic fabric has resulted in a general conclusion that the remanent magnetization fabric is mostly more anisotropic than AMS (Stephenson et al., 1986). Here we show that this is also the case when comparing ferrimagnetic AMS and whole rock AMS. There is however an exception to this rule for the limestone samples, where the F and F_0 fabrics have relatively comparable P' values. This probably indicates that the main part of the F_0 fabric, despite its low susceptibility, is carried by ferrimagnetic minerals.

4.4.1.1. Loess sediments, volcanoclastic sediments and ignimbrite. All samples present a simple enhancement of the F_0 fabric during heating. This evolution corresponds to the model F_0+pF_n or F_0-pF_l. F_0 has shape and axes orientation similar to those of F_n or F_l, but lower P' values than F_n or F_l (i.e. indicating that the new F fabric is related to F_0, but more anisotropic). For the weakly magnetic samples, the bulk susceptibility tensor is determined mainly by the paramagnetic minerals and trace amounts of ferrimagnetic minerals. The simple enhancement of F_0 indicates that the formation of secondary ferrimagnetic minerals occurs by preserving the initial crystal morphology of the paramagnetic and/or antiferromagnetic minerals (precursors). Examples of such pseudomorphic transformations are formation of hematite from goethite dehydroxilation and thermal transformation of lepidocrocite upon heating to maghemite and hematite (Dunlop and Özdemir, 1997). Oxidation of magnetite in air involves a topotactic reaction in which the original crystal morphology is maintained throughout. During heating to temperatures higher than 600 °C, a sintering process leads to formation of irregular hematite particles that differ in morphology from the precursor (Cornell and Schwertmann, 1996). That corresponds to the high temperature heating steps which were discarded because the F fabric obtained at lower temperature is different from that for these high temperature heating steps.

All the samples d1, e1, f1, f2, g1 and g2, present similar F_0 and F fabrics. They also undergo similar mineralogical alterations, with newly formed magnetite or grain size variation, and, at least for some of them, occurrence of hematite at very high temperature (T>600 °C).

4.4.1.2. Limestones and plutonic rocks. In limestones the F fabric is clearly different from the F_0 fabric. The axes permutation suggests, at least for the level 2 samples, that one of the newly formed fabrics is inverse (this will be discussed using remanence anisotropy in the next section). It is clear that the F_0 fabric was not simply enhanced during heating. The fabric of all the plutonic samples (b1–b4 and c1–c4) is also not simply enhanced during heating. For these samples, linear regression indicates that heating introduces a fabric evolution following the models F_0+pF_n or F_0-pF_l. This implies that characteristics of the fabrics F_0 and F_n are in this case different. F_0

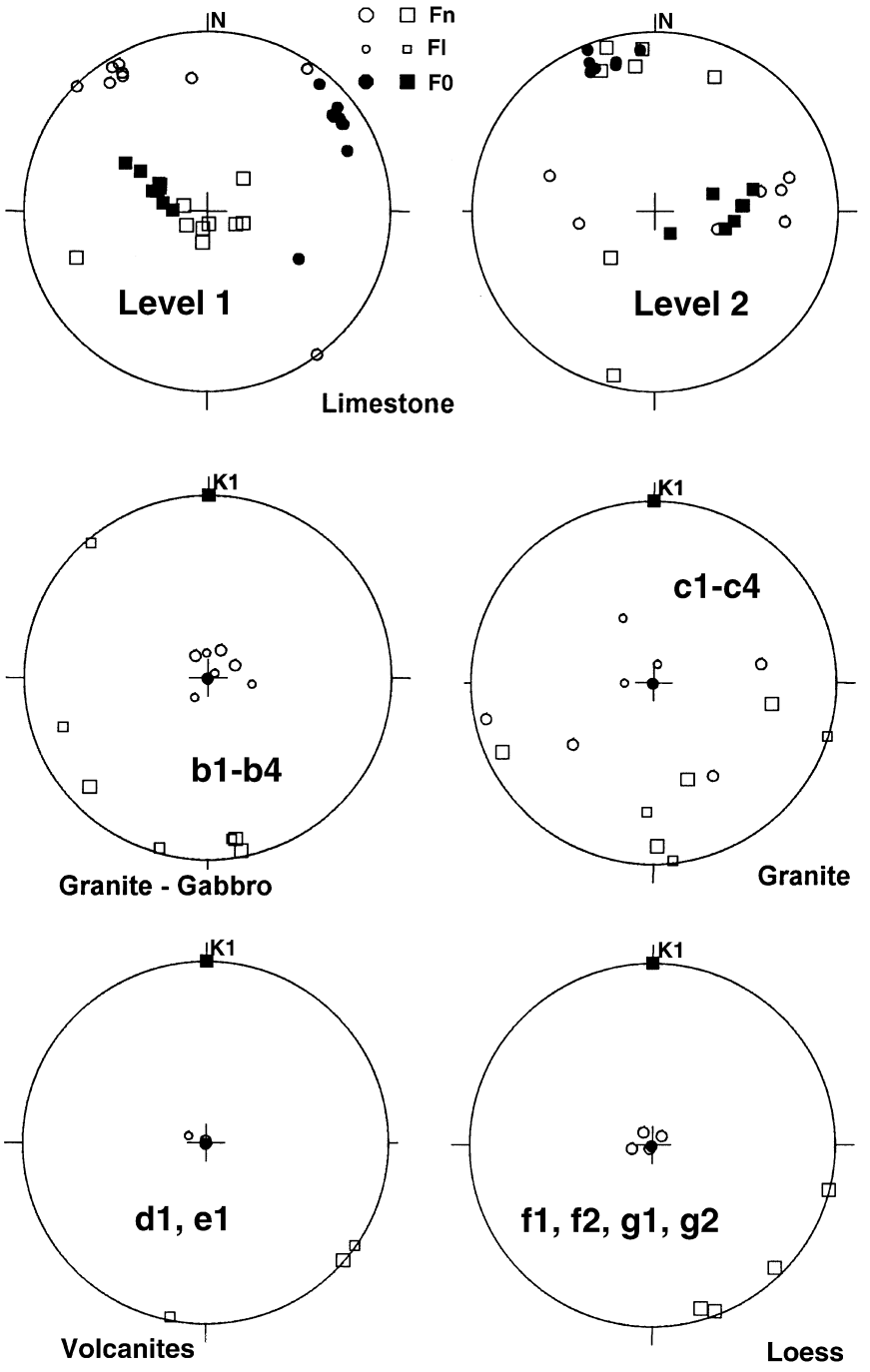

Fig. 7. Maximum (squares) and minimum (circles) susceptibility axes corresponding to the ferrimagnetic minerals formed (large open symbols) or disappeared (small open symbols) during the heating and for whole rock before heating (full symbols). Stereographic projection in the lower hemisphere in geographic coordinates for limestones from levels 1 and 2. For the other samples, coordinates are those of the magnetic fabric before heating: minimum and maximum (K_1) axes respectively vertical and horizontal.

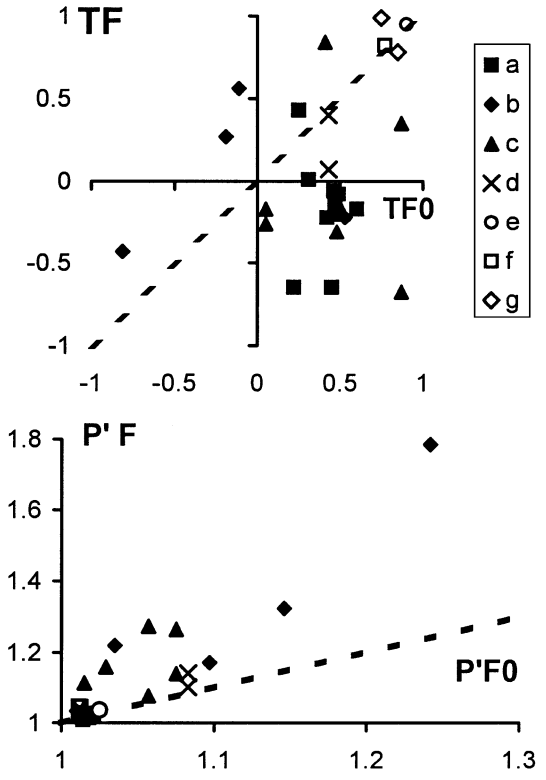

Fig. 8. T and P' parameters values for the ferrimagnetic minerals formed or that have disappeared during the heating (TF and $P'F$) as a function of those for whole rock before heating (TF_0 and $P'F_0$). Dashed line correspond to $TF_0 = TF$ and $P'F_0 = P'T$.

could be mainly carried either by paramagnetic minerals, or by ferrimagnetic minerals with characteristics different from the ferrimagnetic minerals formed or destroyed during heating, or by paramagnetic and ferrimagnetic minerals. The newly formed ferrimagnetic minerals can have a fabric identical or different from that of the ferrimagnetics formed or destroyed during heating. In the case of limestone samples, the rock-magnetic data suggest that the major fraction responsible for the differences in magnetic fabric at different temperature steps is newly formed magnetite. In granite pyrrhotite is transformed above 400 °C to magnetite and hematite.

4.4.2. Comparison of the F fabric with remanence anisotropies

To test the possibility for an inverse AMS fabric related to SD grains, Souque et al. (2002) measured the anisotropies of anhysteretic and isothermal remanent magnetization (AARM and AIRM, respectively) on some of the studied limestones, before any heating and after heating at 500 °C. Despite significant scatter, part of these anisotropies appeared to be coherent with the AMS data (Figs. 7 and 9), and Souque et al. (2002) excluded assumption of an inverse fabric for F_0. The F_0 fabric for level 1 was attributed to a late recrystallization and for level 2 to layer parallel shortening related to the compression.

For level 2, the AARM fabric before heating and the fabric obtained using the tensor difference of the AARM before and after heating (Fig. 9) are similar to the F_0 fabric (Fig. 7), which is therefore not an inverse fabric and is not carried by SD grains. These AARM fabrics present again a permutation of axes maximum–minimum relative to the F fabric. All these observations clearly show that the F fabric is an inverse fabric, therefore carried mainly by SD grains. However, significant tensor differences for the F fabric point out that the evolution during heating is not so simple. Fig. 10 presents the example of sample a25, with occurrence of an inverse fabric from 250 to 350 °C, loss of an inverse fabric between 400 and 450 °C and occurrence of a "normal" fabric at higher temperature. This explains in particular why the data obtained after 500 °C heating were excluded because of lower quality of the regressions.

For level 1, high coercivity AARM fabric before heating and the fabric obtained using the AARM tensor difference (Fig. 9) are similar to the F fabric (Fig. 7). This should indicate that the F fabric is a normal fabric and therefore not carried mainly by SD grains. However, detailed analysis of the tensor difference (sample a19 in Fig. 10) shows complex permutations of axes, probably indicating formation of SD grains at the same time. Low coercivity AARM fabric is not very different from the F_0 fabric. It seems to be intermediate between AIRM and high coercivity AARM. The F_0 fabric is therefore probably a composite fabric, of which the F fabric probably corresponds to one of the components.

4.4.3. Effect of heating on the magnetic fabric

For the samples exhibiting sufficient susceptibility decrease and increase, two different cases have been observed for the corresponding fabrics. For samples d1 and e1 showing during thermal treatment the

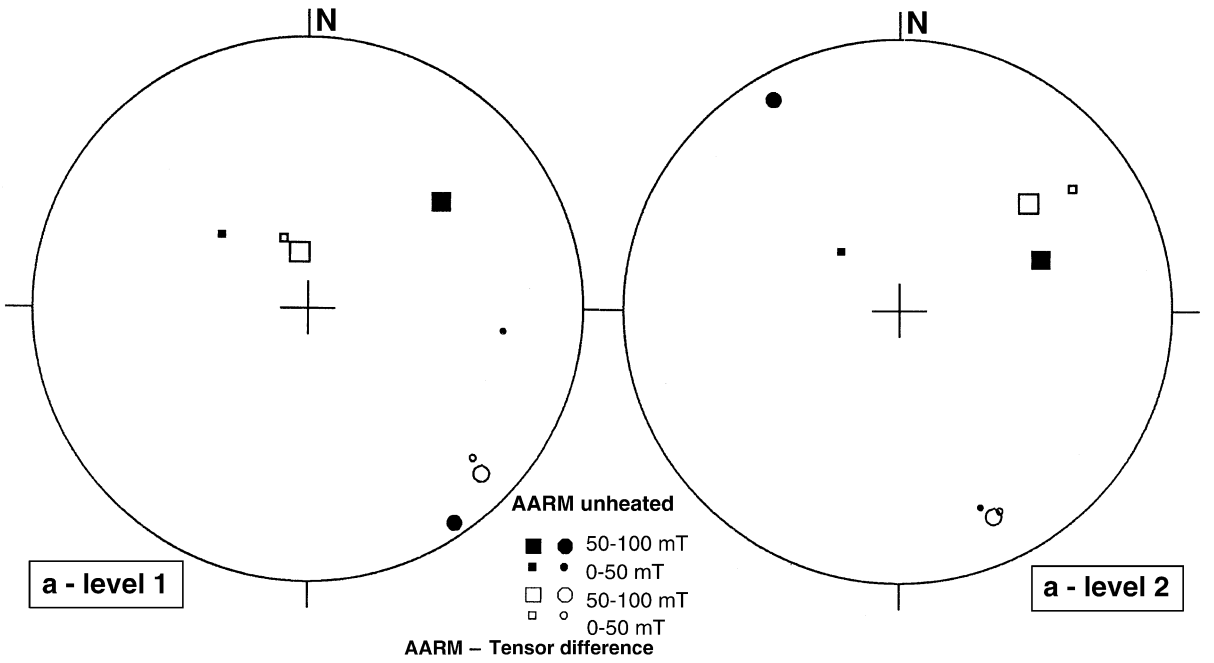

Fig. 9. For limestone samples, mean maximum (squares) and minimum (circles) axes for AARM, before heating (full symbols) and for the AARM tensor difference between 500 °C heated and unheated steps (open symbols). AARM windows 0–50 mT (small symbols) and 50–100 mT (large symbols). Stereographic projection in the lower hemisphere.

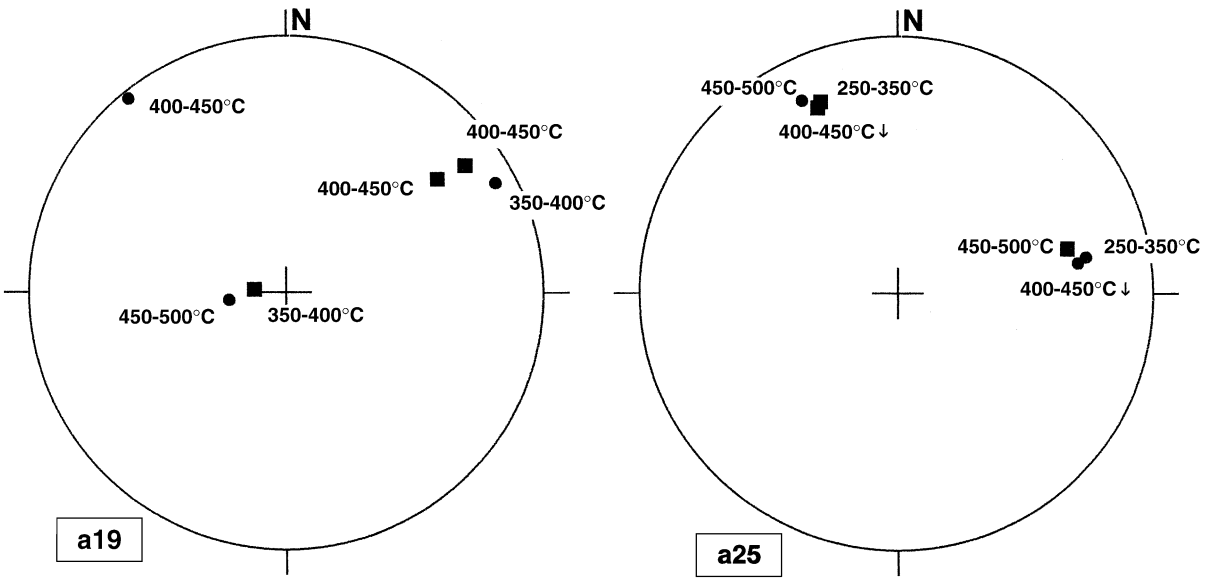

Fig. 10. Maximum (squares) and minimum (circles) susceptibility axes for different tensor differences (indicated with their corresponding window of temperature) for *F* fabric of the limestone samples a19 and a25. Stereographic projection in the lower hemisphere.

susceptibility increase first, the two fabrics—F_n and F_l—are similar. This suggests that grains of the mineral formed at the beginning are similar to grains of the mineral destroyed at higher temperature. That could be due to the formation of magnetite in the medium temperature range that is subsequently oxidized to hematite at higher temperatures. For samples c1, c3 and c4 showing during thermal treatment the susceptibility decrease first, the two fabrics F_n and F_l are different (Fig. 11). Consequently, the grains that disappear at low temperatures are not replaced by grains with similar fabric at higher temperatures. Precisely, all the studied granite samples present mineralogical alterations with magnetite forming from pyrrhotite. The two different F fabrics could be therefore carried by different minerals—pyrrhotite and magnetite.

Heating therefore does not always yields simple fabric enhancement. The resultant fabric is sometimes the inverse of the initial fabric, or has differently oriented axes. It is obvious that the studied samples are not representative of all sedimentary, volcanic or plutonic rocks. There are probably granites undergoing simple enhancement of the fabric and loess with F fabric different from F_0.

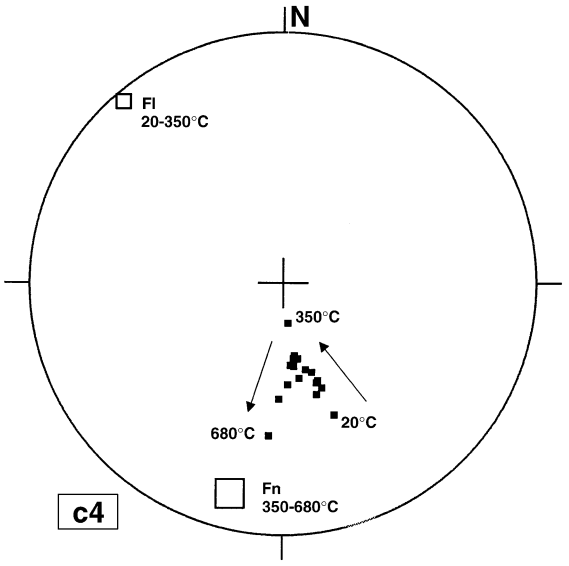

Fig. 11. For the granite sample c4, maximum susceptibility axes for the ferrimagnetic minerals formed (large open symbol) or disappearing (small open symbol) during the heating, and measured for whole rock (small full symbol) after each step of the thermal treatment. Arrows indicate the variation of the axis orientation for increasing temperature steps. Stereographic projection in the lower hemisphere. Temperature in °C.

5. Conclusions

Both cases of simple enhancement and of highlighting of different masked fabrics have been obtained in our test samples. The use of heating therefore cannot be generalized to simply enhance a particular magnetic fabric. It must be accompanied by an analysis of how the AMS varies in order to attain a reliable interpretation. Masked fabrics could allow very useful structural information. Systematic AMS measurements during thermal demagnetization could allow the obtaining of such data and, for a selected sample set, should become a standard procedure.

When the fabric of the ferrimagnetic minerals gained or lost during thermal treatment is similar for different thermal steps, it is clear that these ferrimagnetic minerals are not randomly oriented. Standard heating procedure is carried out in a zero magnetic field, thus the fabric of these ferrimagnetic minerals cannot be related to an ambient magnetic field (cf. Pick and Tauxe, 1991). The pre-existing minerals should therefore determine the orientation of these ferrimagnetic minerals. Indeed, these ferrimagnetic minerals either simply replace pre-existing minerals (or are replaced by minerals of lower susceptibility) or correspond to exsolution from pre-existing minerals. The shape of such exsolved ferrimagnetic minerals is mostly controlled by the crystal lattice or the surface of the pre-existing minerals. These ferrimagnetic minerals then have a fabric, which mimics the fabric of the pre-existing minerals (possibly sometimes distribution anisotropy; Hargraves et al., 1991). Coherent AMS of ferrimagnetic minerals formed or lost during thermal treatment is therefore related to the fabric of one mineral-type or of several families of minerals in the rock. If the AMS of ferrimagnetic minerals is similar to the initial fabric, heating gives a simple enhancement of this fabric. If this AMS is different, heating will cause changes other than a simple enhancement. AMS of ferrimagnetic minerals formed or destroyed during thermal treatment reveals the fabric of some minerals of the rock. This fabric was revealed because of the low anisotropy of these

minerals compared to that of the main carriers of the initial whole rock fabric. Study of AMS during progressive heating thus allows one mostly to isolate components of a composite fabric. The new revealed fabric can correspond to any type of pre-existing structure, e.g. stratification, paleocurrent direction, cleavage, lineation, microcracks or stylolite.

Acknowledgements

This work was supported by Bulgarian Academy of Sciences (BAS) and French CNRS in the framework of bilateral project CNRS-BAS. We are very grateful to M. Bina for his help in rock magnetism, to S. Gilder for help with the manuscript and to M. Dekkers and an anonymous reviewer for constructive comments.

References

Abouzakhm, A.G., Tarling, D.H., 1975. Magnetic anisotropy and susceptibility from northwestern Scotland. J. Geol. Soc. (Lond.) 131, 983–994.

Bina, M., Henry, B., 1990. Magnetic properties, opaque mineralogy and magnetic anisotropies of serpentinized peridotites from ODP hole 670A near Mid-Atlantic ridge. Phys. Earth Planet. Inter. 65, 88–103.

Bina, M., Corpel, J., Daly, L., Debeglia, N., 1991. Transformation de la pyrrhotite en magnetite sous l'effet de la temperature: une source potentielle d'anomalies magnétiques. Compt. Rend. Acad. Sci. Paris 313 (II), 487–494.

Borradaile, G.J., Lagroix, F., 2000. Thermal enhancement of magnetic fabrics in high grade gneisses. Geophys. Res. Lett. 27 (16), 2413–2416.

Campbell, A.S., Schwertmann, U., Campbell, P.A., 1997. Formation of cubic phases on heating ferrihydrite. Clay Miner. 32, 615–622.

Constable, C., Tauxe, L., 1990. The bootstrap for magnetic susceptibility tensors. J. Geophys. Res. 95, 8383–8395.

Cornell, R.M., Schwertmann, U., 1996. The Iron Oxides. Structure, Properties, Reactions, Occurrence and Uses. Weinheim, VCH Verlagsgesellschaft.

Dekkers, M.J., 1990a. Magnetic monitoring of pyrrhotite alteration during thermal demagnetisation. Geophys. Res. Lett. 17, 779–782.

Dekkers, M.J., 1990b. Magnetic properties of natural goethite: III. Magnetic behaviour and properties of minerals originating from goethite dehydration during thermal demagnetisation. Geophys. J. Int. 103, 233–250.

Dunlop, D.J., Özdemir, Ö., 1997. Rock Magnetism. Fundamentals and Frontiers. Cambridge Univ. Press., Cambridge. 573 pp.

Efron, B., 1982. The jackknife, the bootstrap and other resampling plans. SIAM. Reg. Conf. Ser. App. Math., vol. 38. Philadelphia.

Efron, B., Tibshirani, R., 1986. Bootstrap methods for standard errors, confidence intervals, and other measures of statistical accuracy. Stat. Sci. I, 54–77.

Ellwood, B.B., Balsam, W., Burkart, B., Long, G.J., Buhl, M.L., 1986. Anomalous magnetic properties in rocks containing the mineral siderite: paleomagnetic implications. J. Geophys. Res. 91, 12779–12790.

Gehring, A.U., Heller, F., 1989. Timing of natural remanent magnetization in ferriferous limestones from the Swiss Jura mountains. Earth Planet. Sci. Lett. 93, 261–272.

Gehring, A.U., Hofmeister, A.M., 1994. The transformation of lepidocrocite during heating: a magnetic and spectroscopic study. Clays Clay Miner. 42 (4), 409–415.

Hargraves, R.B., Johnson, D., Chan, C.Y., 1991. Distribution anisotropy: the cause of AMS in igneous rocks? Geophys. Res. Lett. 18, 2193–2196.

Hartstra, R.L., 1982. Grain size dependence of initial susceptibility and saturation magnetization-related parameters of four natural magnetites in the PSD-MD range. Geophys. J. R. Astr. Soc. 71, 477–495.

Henry, B., 1983. Interprétation quantitative de l'anisotropie de susceptibilité magnétique. Tectonophysics 91, 165–177.

Henry, B., 1997. Bootstrap and magnetic fabric. EUG 9 Meeting, Strasbourg.

Henry, B., Daly, L., 1983. From qualitative to quantitative magnetic anisotropy analysis: the prospect of finite strain calibration. Tectonophysics 98, 327–336.

Hext, G., 1963. The estimation of second-order tensors, with related tests and designs. Biometrika 50, 353.

Hirt, A.M., Gehring, A.U., 1991. Thermal alteration of the magnetic mineralogy in ferruginous rocks. J. Geophys. Res. 96, 9947–9953.

Hus, J., Jordanova, D., 1996. The "Blake Event" recorded in an Early Weischelian loess deposit at Tönchesberg East Eifel volcanic field (Germany)? Geol. Carpath. 47, 186–187.

Jelenska, M., Kadziako-Hofmokl, M., 1990. Dependence of anisotropy of magnetic susceptibility of rocks on temperature. Phys. Earth Planet. Int. 62, 19–31.

Jelinek, V., 1978. Statistical processing of magnetic susceptibility measured in groups of specimens. Stud. Geophys. Geod. 22, 50–62.

Jelinek, V., 1981. Characterization of the magnetic fabric of rocks. Tectonophysics 79, 63–67.

Karloukovski, V., 2000. Magnetostratigraphy and palaeomagnetism of the area around the Momchilgrad Palaeogene depression, the East Rhodope massif. PhD thesis, University of East Anglia, Norwich.

Kropacek, V., 1976. Changes of magnetic susceptibility and its anisotropy of basalts by oxidation of titanomagnetites. Stud. Geophys. Geod. 20, 178–185.

Li, X.Z., Dobson, J., Chen, Z., Chang, W.J., St. Pierre, T.G., 1998. Multimodal investigation of thermally induced changes in magnetic fabric and magnetic mineralogy. Geophys. J. Int. 135, 988–998.

Lowrie, W., 1990. Identification of ferromagnetic minerals in a rock by coercivity and unblocking temperature properties. Geophys. Res. Lett. 17, 159–162.

Murad, E., Wagner, U., 1998. Clays and clay minerals: the firing process. Hyperfine Interact. 117, 337–356.

Osipov, J., 1978. Magnetism of Clay Soils (in Russian). Nedra, Moscow.

Özdemir, Ö., 1990. High temperature hysteresis and thermoremanence of single-domain maghemite. Phys. Earth Planet. Inter. 65, 125–136.

Peraneau, A., Tarling, D.H., 1985. Thermal enhancement of magnetic fabric in Cretaceous sandstones. J. Geol. Soc. (Lond.) 142, 1029–1034.

Pick, T., Tauxe, L., 1991. Chemical remanent magnetization in synthetic magnetite. J. Geophys. Res. 96, 9925–9936.

Riccardi, M., Messiga, B., Dominuco, P., 1999. An approach to the dynamics of clay firing. Appl. Clay Sci. 15, 393–409.

Schultz-Krutisch, T., Heller, F., 1985. Measurements of magnetic susceptibility anisotropy in Bundsandstein deposits from Southern Germany. J. Geophys. 57, 51–58.

Schwartz, E.J., Vaughan, D.J., 1972. Magnetic phase relations of pyrrhotite. J. Geomagn. Geoelectr. 24, 441–458.

Souque, C., Robion, P., Frizon de Lamotte, D., 2002. Cryptic magnetic fabric of tectonic origin revealed by heating of sedimentary samples from the Corbières (France). Phys. Chem. Earth 27, 1253–1262.

Stacey, F.D., Banerjee, S.K., 1974. The Physical Principles in Rock Magnetism. Elsevier, Amsterdam. 195 pp.

Stephenson, A., Sadikum, S., Potter, D.K., 1986. A theoretical and experimental comparison of the anisotropies of magnetic susceptibilty and remanence in rocks and minerals. Geophys. J. R. Astron. Soc. 84, 185–200.

Tauxe, L., Watson, G.S., 1994. The fold test: an eigen analysis approach. Earth Planet. Sci. Lett. 122, 331–341.

Trincade, R.I.F., Mintsa Mi Nguema, T., Bouchez, J.L., 2001. Thermally enhanced mimetic fabric of magnetite in a biotite granite. Geophys. Res. Lett. 28, 2687–2690.

Urrutia-Fucugauchi, J., 1981. Preliminary results on the effects of heating on the magnetic susceptibility anisotropy of rocks. J. Geomagn. Geoelectr. 33, 411–419.

Van Velzen, A.J., Zijderveld, J.D.A., 1992. A method to study alterations of magnetic minerals during thermal demagnetization applied to a fine-grained marine marl (Trubi formation, Sicily). Geophys. J. Int. 110, 79–90.

Verwey, 1935. Crystal structure of γFe_2O_3 and γAl_2O_3. Z. Kristallogr. 91, 65–69.

Weidler, P., Stanjek, H., 1998. The effect of dry heating of synthetic 2-line and 6-line ferrihydrite: II. Surface area, porosity and fractal dimension. Clay Miner. 33, 277–284.

Xu, T.C., Ye, S.J., Yang, F., 1991. A preliminary study of thermally enhanced magnetic fabric in the Tertiary sediments from Qaidam basin, NW China. Stud. Geophys. Geod. 35, 295–301.